Supplemental Information for

Plasticity of Renal Erythropoietin-Producing Cells Governs Fibrosis

Tomokazu Souma, Shun Yamazaki, Takashi Moriguchi, Norio Suzuki, Ikuo Hirano, Xiaoqing Pan, Naoko Minegishi, Michiaki Abe, Hideyasu Kiyomoto, Sadayoshi Ito, and Masayuki Yamamoto*

*To whom correspondence should be addressed. E-mail: masiyamamoto@med.tohoku.ac.jp

This PDF file includes 8 supplementary figures and 1 supplementary table.

SUPPLEMENTAL METHODS

Unilateral Ischemia Reperfusion Injury (IRI) Model

The left renal pedicle was exposed and clamped by a vascular clip for 30 minutes. Then, mice were sacrificed 14 days after IRI. Contralateral kidneys were used as controls.

Protein Overload Nephropathy Model

Mice were intraperitoneally injected with oleic acid-conjugated bovine serum albumin (0.3 g) or PBS daily for 7 consecutive days. For the preparation of oleic acid-conjugated albumin, oleic acid (Sigma) was added to sterile albumin (Sigma) solution at a molar ratio of 3:1 (OA:Alb), then incubated at 37°C for 2.5 hrs[1]. The kidneys from PBS injected group were used as controls.

Western Blotting

Homogenates of kidneys were diluted in 2x sample buffer, separated by SDS-PAGE, transferred to PVDF membrane, and immunoblotted with antibodies against GFP (MBL) and α-tubulin (Sigma).

SUPPLEMENTAL FIGURES

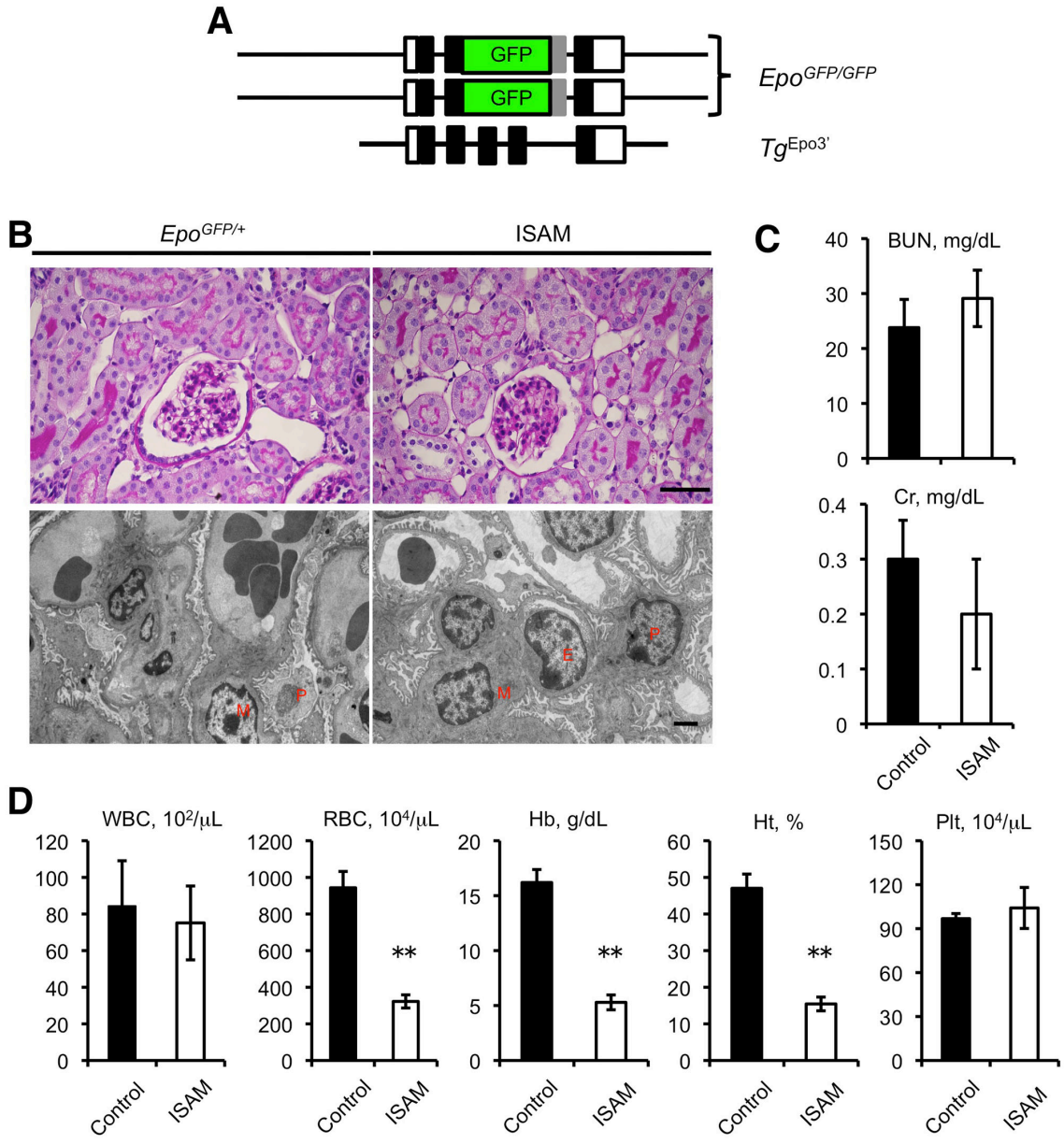

Supplemental Figure 1. ISAM shows severe anemia in adulthood without renal abnormalities. (**A**) Structures of Epo-expressing transgene (*Tg*$^{Epo3'}$) and *Epo*-knockout/GFP-knock-in alleles (*Epo*$^{GFP/GFP}$). (**B**) Histology of ISAM kidneys. Histological analyses (upper panels; Periodic acid-Schiff staining, lower panels; electron micrograph) of kidneys were performed using kidneys of *Epo*$^{GFP/+}$ and ISAM, showing no gross abnormalities. Scale Bars: 50 μm (upper panels) and 2 μm (lower panels). (**C**) Renal function test. (**D**) Hematological indices. Normocytic normochromic anemia was observed in ISAM. *Epo*$^{GFP/+}$::*Tg*$^{Epo3'}$ littermate mice were used as a control (**C**, **D**; Control). $^{**}P<0.01$. Abbreviations: M, mesangial cell; P, podocyte; E, endothelial cell; BUN, blood urea nitrogen; Cr, creatinine; WBC, white blood cell count; RBC, red blood cell count; Hb, hemoglobin; Ht, Hematocrit; and Plt, platelet.

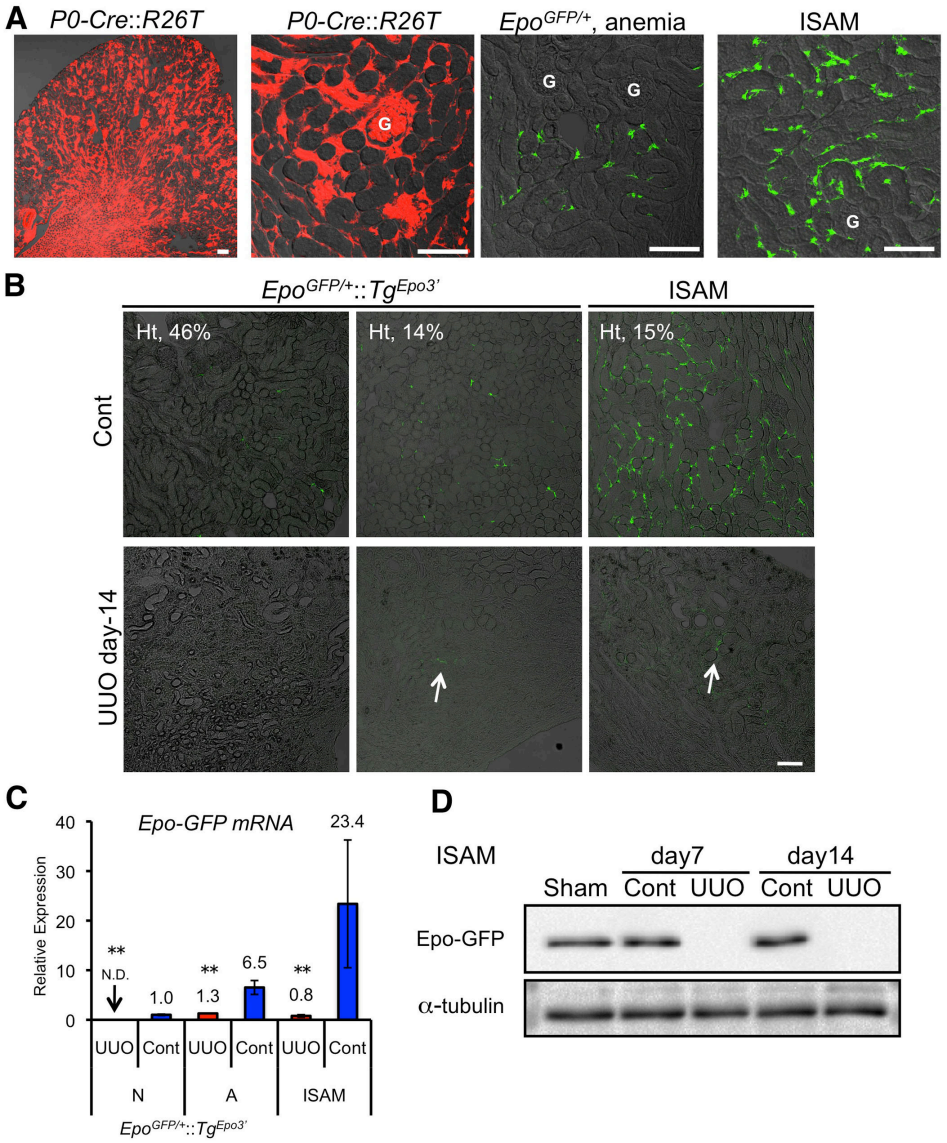

Supplemental Figure 2. ISAM offers specific and efficient monitoring of REPs. (**A**) P0-Cre labeled all renal interstitial cells and glomeruli (G), and also some tubular cells (red, left two panels). Epo-GFP-positive cells (REPs) in *Epo*$^{GFP/+}$ mice were only a minor population of renal interstitial cells under the anemic stimuli using phlebotomy (green, third panel). The number of Epo-GFP-positive cells (G-REPs) in ISAM was markedly increased (green, rightmost panel). (**B**) Distribution of REPs at UUO day-14. Immunohistochemical analyses were performed for *Epo-GFP* expression. White arrows indicate REPs in UUO-treated kidneys. Note that most of renal fibroblasts lost their Epo-producing ability even in the severe anemic conditions. (**C**) Fibrotic kidneys lose anemia-inducible Epo-producing ability. Real-time PCR analyses were performed to quantify *Epo-GFP* mRNA levels using kidneys underwent UUO at day-14. *Epo-GFP* levels were divided by 2 in ISAM to normalize the number of *Epo-GFP* alleles. (**D**) Loss of Epo-producing potentials upon unilateral ureteral obstruction (UUO). Western blotting was performed using whole kidney homogenates of ISAM that underwent Sham or UUO treatments. Note that expression levels of Epo-GFP in UUO-treated kidneys are negligible compared with Sham and contralateral (Cont) kidneys. **, $P<0.01$ vs. Cont kidneys of each conditions. Scale bars: 100 μm. Abbreviation: R26T, *Rosa26-tdTomato*. R26T is a more efficient reporter line than the mice we used previously, *R26R*[2]. The tdTomato fluorescence (red) indicates the recombination of *R26T* locus (See Figure 2C); Cont, contralateral; Ht, Hematocrit; N, normal (Ht, 46%); A, anemic (Ht, 14%) by phlebotomy.

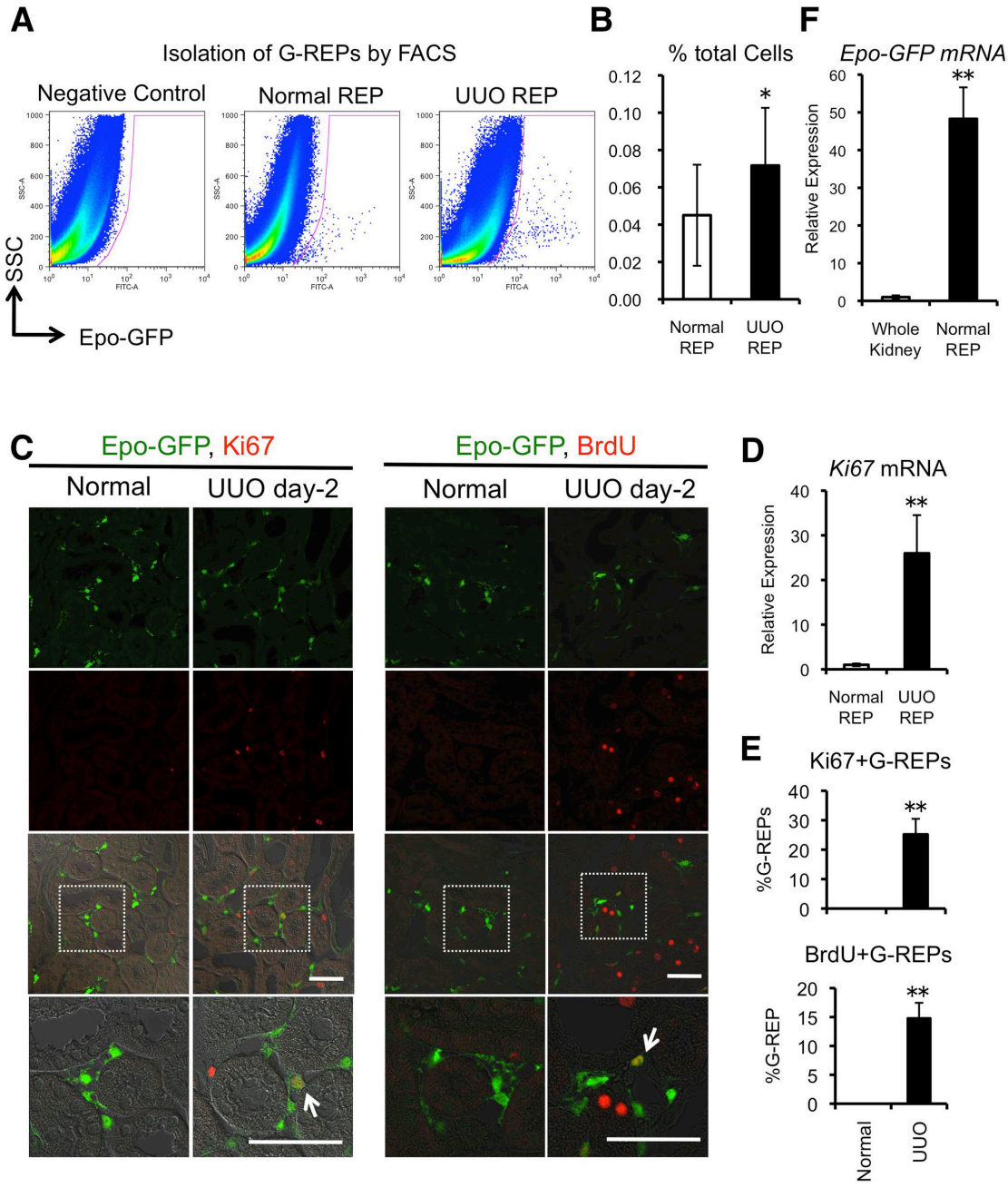

Supplemental Figure 3. REPs proliferate upon UUO. (**A** and **B**) Increased number of G-REPs upon UUO. FACS analyses were performed to count the number of G-REPs in UUO-treated (day-2) and normal ISAM kidneys. A single cell suspension of kidneys from wild type mice were used as a negative control for GFP fluorescence. The number of G-REPs was increased at 2 days after UUO. (**C**) Proliferation of G-REPs upon UUO. Immunofluorescent staining was performed for Epo-GFP (green), and Ki67 or BrdU (red) to detect proliferating G-REPs. White arrow indicates overlapping expression of Ki67 (a marker of cell cycle entry) or BrdU with Epo-GFP (yellow) in the nucleus. Ki67-positive or BrdU-incorporated G-REPs were observed at day-2 after UUO procedure. Scale Bars: 50 μm. (**D** and **E**) Quantitative analyses of proliferation of G-REPs. *Ki67* mRNA levels were analyzed by real-time PCR using FACS-sorted G-REPs in (D). Ki67–positive G-REPs and BrdU-incorporated G-REPs were counted in (E). (**F**) Validation of FACS-sorting of G-REPs. *Epo-GFP* mRNA levels were analyzed by real-time PCR using FACS-sorted REPs and whole kidneys of ISAM. *, $P<0.05$ and **, $P<0.01$. Abbreviation: SSC, side scatter.

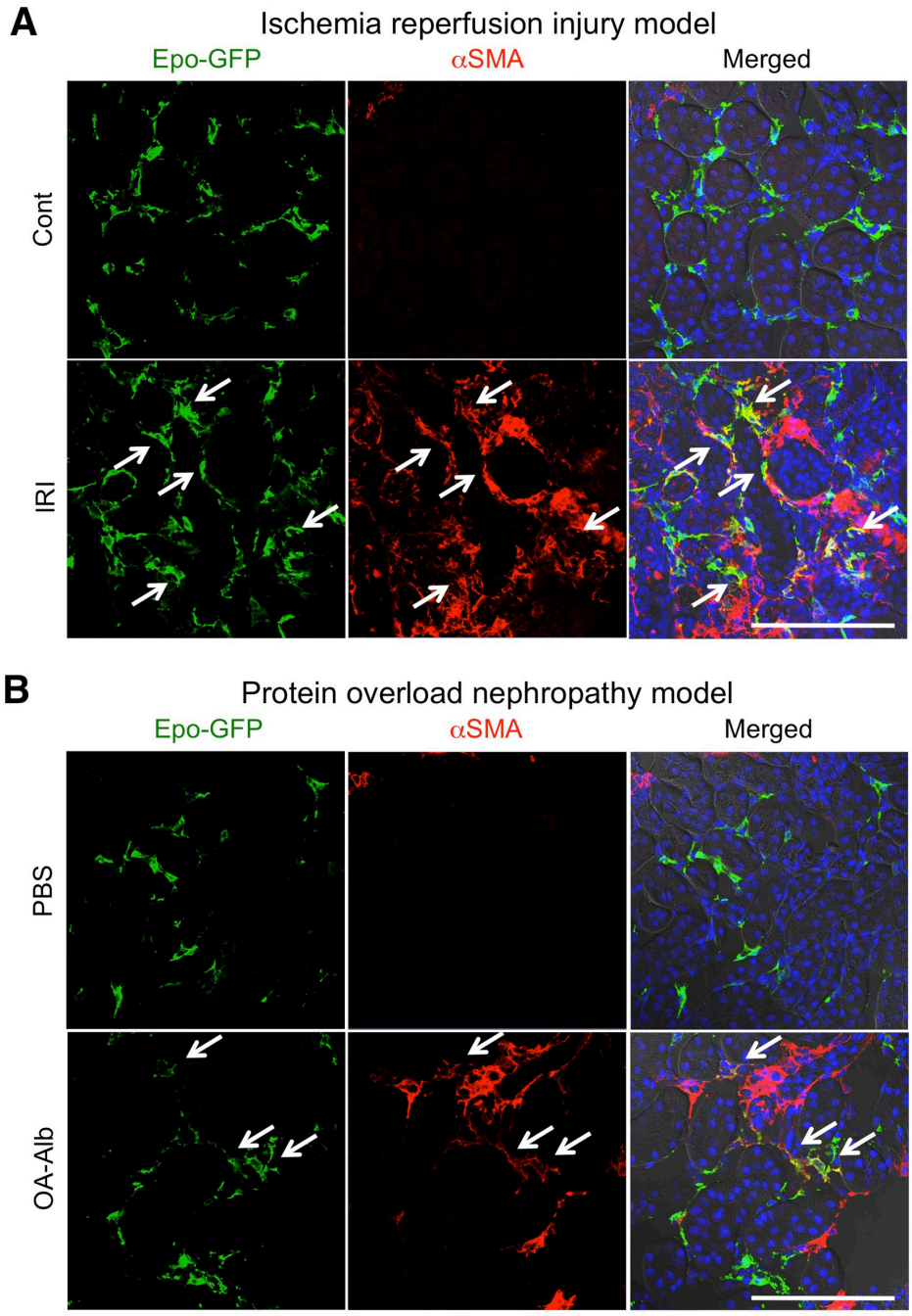

Supplemental Figure 4. Myofibroblastic transformation of G-REPs is a common pathological pathway of kidney injury. Immunofluorescent staining was performed for Epo-GFP (green), αSMA (red), and nucleus (blue) of kidneys from ISAM underwent either (**A**) ischemia reperfusion injury model or (**B**) protein overload nephropathy model. White arrows indicate αSMA-positive G-REPs. Scale bars: 100 μm. Abbreviations: OA-Alb, albumin with oleic acid; IRI, ischemia reperfusion injury; Cont, contralateral kidney.

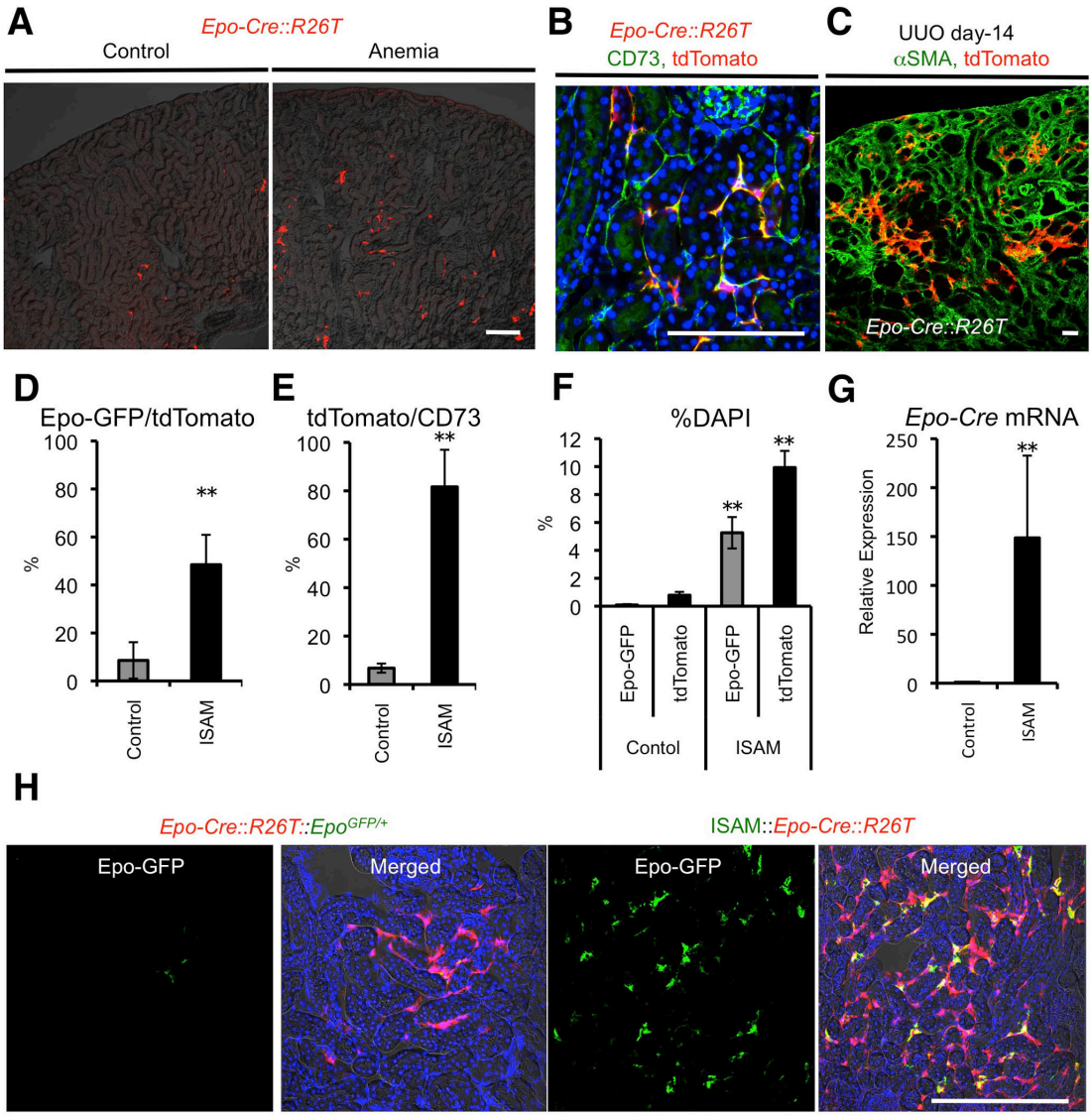

Supplemental Figure 5. Characterization of *Epo-Cre* mice using R26T reporter mice. (**A**) Distribution of Epo-Cre cells. Note that tdTomato fluorescence (red) shows characteristic juxta-medullary distribution of REPs (control), which expand with anemic stimuli (anemia). (**B**) Expression of a commonly used marker of REPs in Epo-Cre cells. Note that tdTomato fluorescence (red; Epo-Cre cells) is overlapped with immunofluorescence of CD73 (green) in kidneys from *Epo-Cre*::*R26T* mice. Nucleus was stained with DAPI (blue). (**C**) αSMA expression of Epo-Cre cells in UUO-treated kidneys. tdTomato (red; Epo-Cre cells) fluorescence and αSMA (green) immunofluorescence were analyzed using kidneys from *Epo-Cre*::*R26T* mice that underwent UUO (day-14). Note that almost all cortical and outer medullary fibroblast-like cells were positive for αSMA. The overlapping expression of tdTomato and αSMA was observed around the juxta-medullary area of UUO-treated kidneys (yellow-orange). (**D-F**) Quantitative characterization of G-REPs and Epo-Cre cells. Immunohistochemical analyses were performed to count the numbers of Epo-GFP^{+} cells (G-REPs), tdTomato^{+} cells (Epo-Cre cells), interstitial CD73^{+} cells, and total cells (DAPI) in cortex and outer medulla of kidneys in control (*Epo-Cre*::*R26T*) and ISAM (ISAM::*Epo-Cre*::*R26T*) conditions. Hematocrit levels of control and ISAM are 14.9% and 44.3%, respectively. (n=3) (**G**) Transgenic *Epo-Cre* expression is dependent on anemic stimuli. *Epo-Cre* mRNA levels were analyzed by real-time PCR. (**H**) Distributions of G-REPs and Epo-Cre cells. **, P <0.01 vs. control mice. Scale bars: 100 μm.

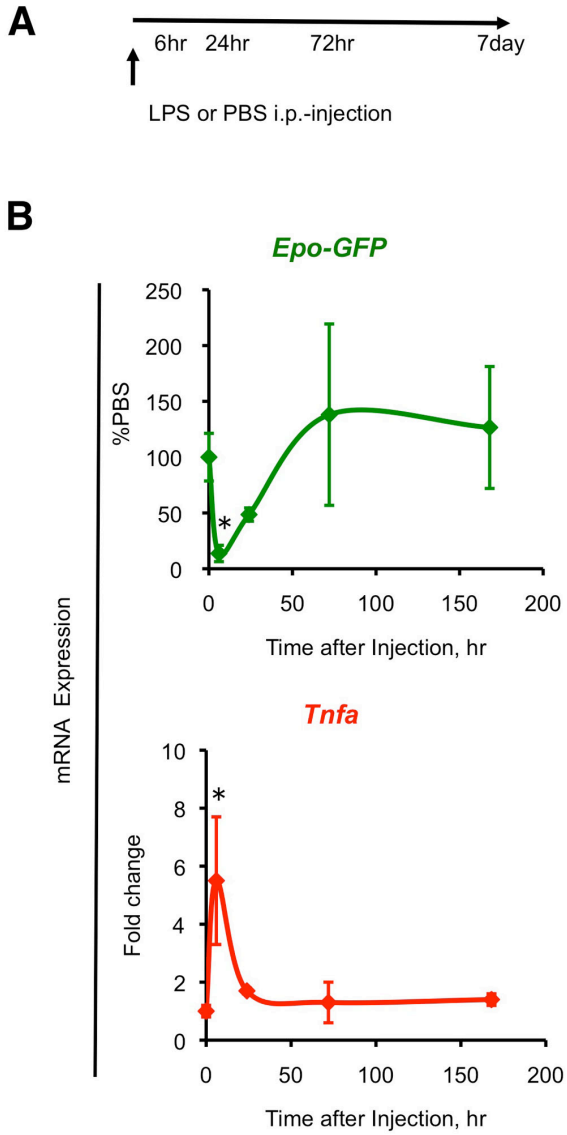

Supplemental Figure 6. LPS-induced repression of Epo-producing potential is reversible. (**A** and **B**) Time-course of *Epo-GFP* and *Tnfa* expressions upon LPS-treatment. Real-time PCR analyses for *Epo-GFP* and *Tnfa* was performed using the kidneys of ISAM that received a single intraperitoneal (i.p.) injection of LPS or PBS. Data of the PBS-injected group were used as the starting point (0 hr). **P*<0.05 vs. PBS-injected group (n>3 per groups).

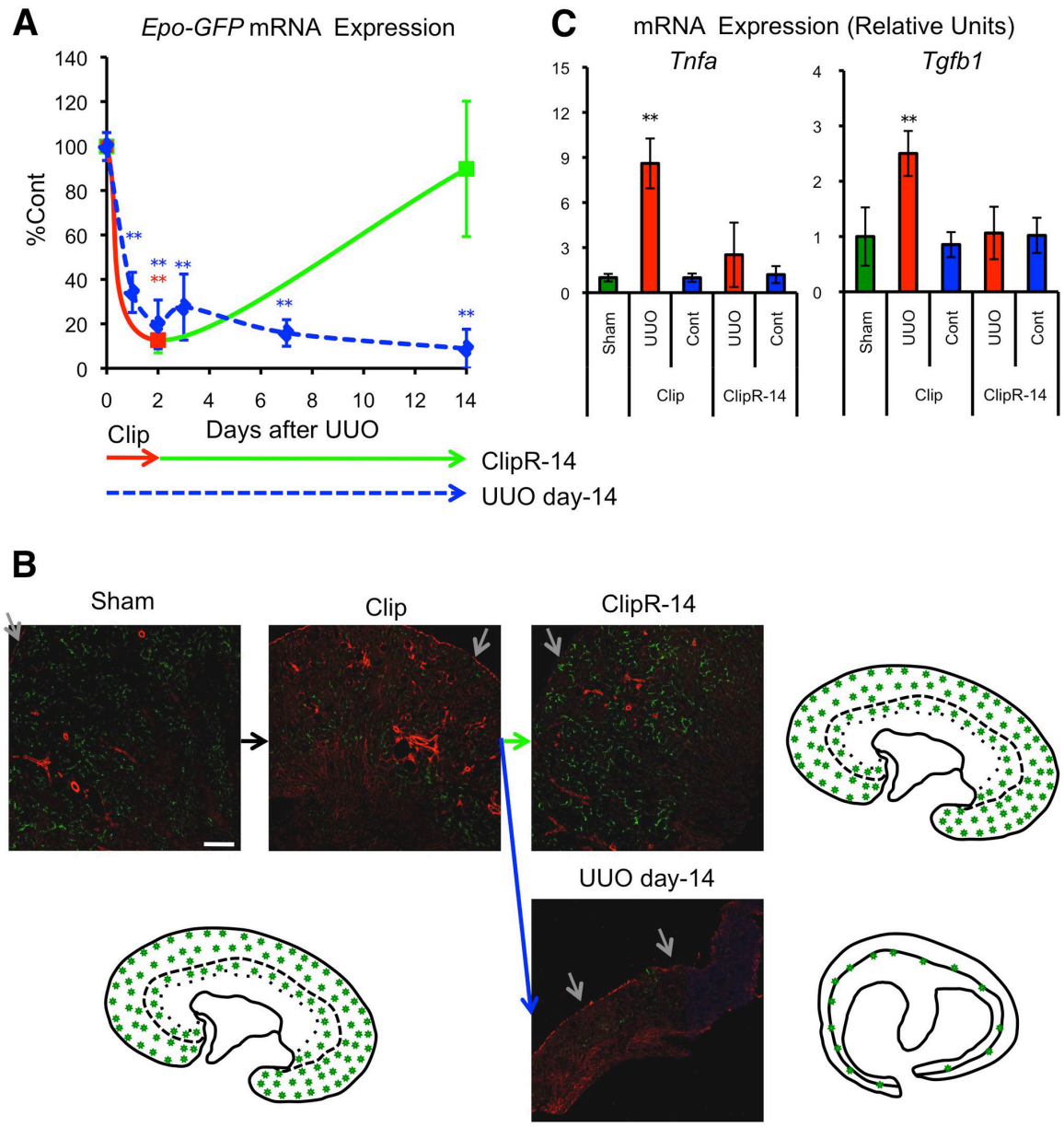

Supplemental Figure 7. Distribution of G-REPs is altered by UUO insults and recovered by reopening the obstruction. (**A**) Time-course of *Epo-GFP* mRNA expression upon UUO. UUO-treatment repressed *Epo-GFP* mRNA expression, but reopening the ureter restored the expression to the control level, indicating that transcription of the *Epo-GFP* was reinitiated after clip removal. Data of the sham-treated group were used as the starting point (day-0), and set as 100%. **, $P<0.01$, n>4. (**B**) Distribution pattern of G-REPs upon UUO. Immunofluorescence analyses were performed for Epo-GFP (green) and αSMA (red). Schematic presentations indicate the distribution of G-REPs (green stars). Normal G-REPs distributed throughout the cortex and outer medulla outer stripe (Sham). UUO insult narrowed the distribution to the cortico-medullary junctions (UUO day-14). The distribution pattern of G-REPs in ClipR-14 kidneys was not distinguishable compared with that in Sham-treated kidneys. The gray arrow indicates the renal capsule. Scale bar: 200 μm. (**C**) Changes of *Tgfb1* and *Tnfa* mRNA levels during Clip-ClipR treatment. Real-time PCR analyses were performed to quantify mRNA expressions using kidneys of Sham, Clip, and ClipR-14 groups. **$P<0.01$ vs. Sham and Cont kidneys (n=5 per group).

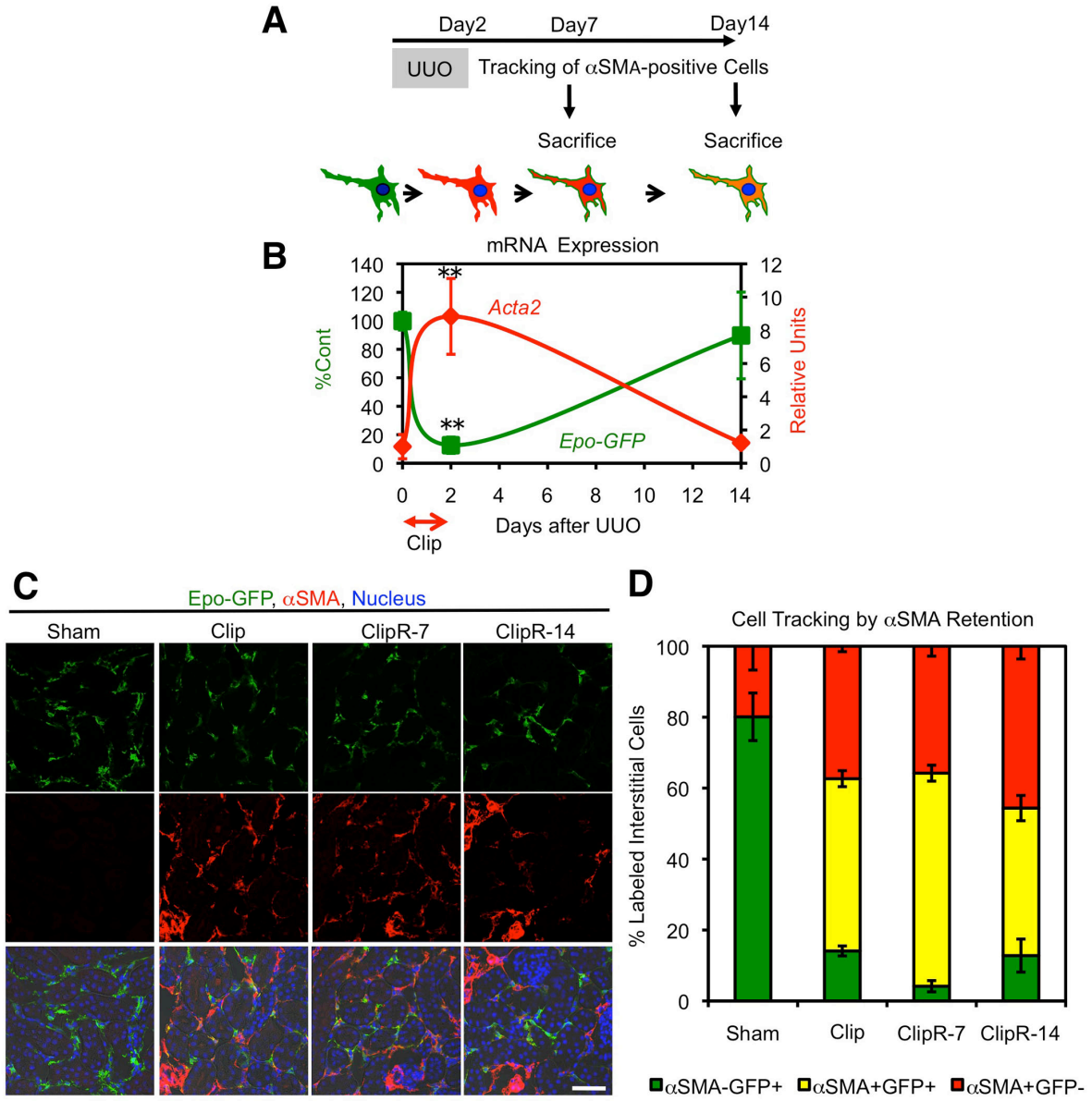

Supplemental Figure 8. Residual αSMA expression allows efficient cell fate tracking of G-REPs. (**A**) Schematic representation of the cell fate tracking strategy. UUO-induced transient accumulation of αSMA protein was used for the cell fate tracking. (**B**) Time-course of *Epo-GFP* and *Acta2* mRNA expression. Reversal of clipping the ureter restored *Epo-GFP* expression to normal level, and terminated *Acta2* transcription. Data of the sham-treated group were used as the starting point (day-0), and set as 100% (*Epo-GFP*) or 1 (*Acta2*). **, $P<0.01$. (**C**) Detection of residual αSMA expression in G-REPs upon Clip-ClipR treatment. Immunofluorescent staining was performed for Epo-GFP (green) and αSMA (red), and nucleus was stained with DAPI (blue). Note that αSMA is continuously positive in most G-REPs throughout Clip-ClipR treatment, and αSMA expression level is decreased in ClipR-14 kidneys (n=3 per group). Scale Bar: 50 μm. (**D**) Efficacy of the cell tracking by using αSMA-retention. αSMA-positive G-REPs were counted in five independent fields (n≥3 per group). Around 77–94 % (yellow) of total G-REPs (green and yellow) were labeled with αSMA after UUO. The αSMA-positive and GFP-negative cells (red) include myofibroblasts and vascular smooth muscle cells.

SUPPLEMENTAL TABLE

Supplemental Table 1. Primers used in this study

Real-time PCR primers

Gene	Sense primer	Antisense primer
Epo-GFP	GGTGGATCCTAAAGCAGCAG	GAAGACTTGCAGCGTGGAC
Acta2	CCCACCCAGAGTGGAGAA	ACATAGCTGGAGCAGCGTCT
Col1a1	AGACATGTTCAGCTTTGTGGAC	GCAGCTGACTTCAGGGATG
Col3a1	TCCCCTGGAATCTGTGAATC	TGAGTCGAATTGGGGAGAAT
Hif1a	CCTGCACTGAATCAAGAGGTTGC	CCATCAGAAGGACTTGCTGGCT
Hif2a	GGACAGCAAGACTTTCCTGAGC	GGTAGAACTCATAGGCGAGCG
Arnt	TGCCTCATCTGGTACTGCTG	TGTCCTGTGGTCTGTCCAGT
Serpine1	AGGATCGAGGTAAACGAGAGC	GCGGGCTGAGATGACAAA
Rela	CCCAGACCGCAGTATCCAT	GCTCCAGGTCTCGCTTCTT
Il6	CTGCAAGAGACTTCCATCCAG	AGTGGTATAGACAGGTCTGTTGG
Ccl2	CATCCACGTGTTGGCTCA	GATCATCTTGCTGGTGAATGAGT
Tnfa	ATGAGAAGTTCCCAAATGGCC	CCTCCACTTGGTGGTTTGCTA
Tgfb1	TGGAGCAACATGTGGAACTC	CAGCAGCCGGTTACCAAG
Mmp3	TTGTTCTTTGATGCAGTCAGC	GATTTGCGCCAAAAGTGC
Mmp9	TGTCTGGAGATTCGACTTGAAGTC	TGAGTTCCAGGGCACACCA
Pdgfb	CGGCCTGTGACTAGAAGTCC	GAGCTTGAGGCGTCTTGG
Itgam	ATGGACGCTGATGGCAATACC	TCCCCATTCACGTCTCCCA
Map2	GCTCCAAGTTTCACAGAAGGAG	AGGTTGGTTCAGATCAATATAAATAGG
Dnmt1	AAGAATGGTGTTGTCTACCGAC	CATCCAGGTTGCTCCCCTTG
Dnmt3a	ACACAGGGCCCGTTACTTCT	TCACAGTGGATGCCAAAGG
Dnmt3b	TGAATGACAAGAAAGACATCTCAAG	CGGGTAGGTTACCCCAGAAG
Cre	ACGTTCACCGGCATCAACGT	CTGCATTACCGGTCGATGCA
Ki67	CATCCATCAGCCGGAGTCA	TGTTTCGCAACTTTCGTTTGTG

Real-time PCR primers using a Taqman probe

Gene	Sense primer	Antisense primer	*Probe*
rRNA	CGGCTACCACATCCAAGGAA	GCTGGAATTACCGCGGCT	TGCTGGCACCAGACTTGCCCTC
Epo	GAGGCAGAAAATGTCACGATG	CTTCCACCTCCATTCTTTTCC	TGCAGAAGGTCCCAGACTGAG TGAAAATA

Genotyping primers

Gene	Sense primer	Antisense primer
$Tg^{Epo3'}$	ACAGGAAGGTCTCACATAGCC	TACAGCTAGGAGAGTTGTGTGG
GFP	CTGAAGTTCATCTGCACCACC	GAAGTTGTACTCCAGCTTGTGC
Cre	ACGTTCACCGGCATCAACGT	CTGCATTACCGGTCGATGCA
R26-IKK2ca	GCAAGACAGAAGCTTCACGACTC	GCAATATGGTGGAAAATAAC
R26T	CTGTTCCTGTACGGCATGG	GGCATTAAAGCAGCGTATCC

REFERENCES

1. Souma, T, Abe, M, Moriguchi, T, Takai, J, Yanagisawa-Miyazawa, N, Shibata, E, Akiyama, Y, Toyohara, T, Suzuki, T, Tanemoto, M, Abe, T, Sato, H, Yamamoto, M, Ito, S: Luminal alkalinization attenuates proteinuria-induced oxidative damage in proximal tubular cells. *J Am Soc Nephrol,* 22**:** 635-648, 2011.

2. Asada, N, Takase, M, Nakamura, J, Oguchi, A, Asada, M, Suzuki, N, Yamamura, K, Nagoshi, N, Shibata, S, Rao, TN, Fehling, HJ, Fukatsu, A, Minegishi, N, Kita, T, Kimura, T, Okano, H, Yamamoto, M, Yanagita, M: Dysfunction of fibroblasts of extrarenal origin underlies renal fibrosis and renal anemia in mice. *J Clin Invest,* 121**:** 3981-3990, 2011.